

# Quantum TAP equations

Giulio Biroli<sup>1,2</sup> and Leticia F. Cugliandolo<sup>2,3</sup>

<sup>1</sup>Center for Material Theory, Department of Physics and Astronomy,  
Rutgers University, Piscataway, NJ 08854 USA

<sup>2</sup>Laboratoire de Physique Théorique de l'Ecole Normale Supérieure\*  
24 rue Lhomond, 75231 Paris cedex 05, France.

<sup>3</sup>Laboratoire de Physique Théorique et Hautes Energies, Jussieu,  
4, Place Jussieu, 75252 Paris Cedex 05, France

November 8, 2018

## Abstract

We derive Thouless-Anderson-Palmer (TAP) equations for quantum disordered systems. We apply them to the study of the paramagnetic and glassy phases in the quantum version of the spherical  $p$  spin-glass model. We generalize several useful quantities (complexity, threshold level, etc.) and various ideas (configurational entropy crisis, etc), that have been developed within the classical TAP approach, to quantum systems. The analysis of the quantum TAP equations allows us to show that the phase diagram (temperature-quantum parameter) of the  $p$  spin-glass model should be generic. In particular, we argue that a crossover from a second order thermodynamic transition close to the classical critical point to a first order thermodynamic transition close to the quantum critical point is to be expected in a large class of systems.

LPT-ENS/0033, LPTHE/0034.

---

\*Unité Mixte de Recherche du Centre National de la Recherche Scientifique et de l'Ecole Normale Supérieure.

# 1 Introduction

Glassy systems of extremely diverse types exist in nature. They all share several common features like a very slow, non-equilibrium dynamics. The development of a full theoretical description of the glassy phase is one of the most important challenges in condensed matter physics. A variety of techniques, that range from scaling arguments to mean-field approaches have been, and are still used, with the aim of attempting a satisfactory description of the glassy properties.

One of these techniques is due to Thouless, Anderson and Palmer (TAP) [1], who introduced an approach to classical disordered systems based on the study of a free-energy landscape. The key object is the Legendre transform of the free-energy  $F(\beta) = -\ln Z/\beta$  with respect to a number of order parameters that are sufficient to describe the transition and the different phases in the system. This function behaves as an effective potential whose minima represent different possible phases. In a classical fully-connected Ising model only one order parameter is needed, the global magnetization  $m = \sum_i \langle s_i \rangle / N$ . The two possible minima of  $F(\beta, m)$  correspond to the two possible states of positive and negative magnetization,  $m = \pm m_o(T)$ . Focusing on the Sherrington-Kirkpatrick (SK) mean-field model for spin-glasses, TAP showed that *all* the local magnetizations  $m_i = \langle s_i \rangle$ ,  $i = 1, \dots, N$ , have to be included in order to derive the relevant free-energy landscape. The extremization condition of the TAP free-energy on the  $m_i$ s leads to the TAP equations. It was soon after realized by Bray and Moore [2, 3] that the number of solutions to the TAP equations for the SK model is exponential in the number of spins in the system, for temperatures below the spin-glass transition [4]. A very useful alternative derivation of the TAP equations was given by Plefka [5] who showed that these equations can also be obtained from a power expansion of the Gibbs potential up to second order in the exchange couplings. The advantage of this derivation is twofold: it allows to show convergence of the power expansion for all temperatures and it is easily applicable to other mean-field glassy models. Moreover, Georges and Yedidia [6] showed that the high temperature series, at fixed order parameter, of the free-energy can be used to derive TAP-like equations, and its corrections, for models in finite dimensions or, equivalently, with finite range interactions. The connection between the TAP approach and the more standard analysis of the partition function of a disordered model has been exhibited by De Dominicis and Young [7] who showed that, for the SK model, one recovers the equilibrium results of the replica or the cavity method [8] via weighted Boltzmann averages over solutions of the TAP equations. More recently, the TAP approach has been applied to other classical disordered models. In particular, two models that we shall discuss in the following, the spherical and Ising  $p$  spin-glass models [9, 10, 11, 12, 13, 14] and the Ghatak-Sherrington (GS) model [15, 16] have been analyzed with this method [17, 18, 19].

Glassy systems, and in particular disordered ones, are characterized by having a very slow dynamics with non equilibrium effects at low temperatures [20, 21]. Mean-field models, like the the spherical  $p$  spin-glass model [22] or the SK spin-glass [23], capture this phenomenology. The dynamic solution for the evolution starting from random initial conditions, that represent a quench from high temperatures analytically, is intimately connected to the structure and organization of TAP solutions. One of the most striking

results of the dynamic analysis of  $p$  spin-glass-like models is that the energy density (and other one time-quantities) converges asymptotically to the energy density of high lying solutions of the TAP equations. This level has been called *threshold*. The energy-density in equilibrium is different. This and other related results suggest that an interpretation of the dynamics in terms of a motion in a TAP free-energy landscape can be given [22]. The generalization of the TAP approach to dynamics that has been developed in [24] allows one to make this statement precise: the evolution is determined by a gradient-descent in the TAP free-energy landscape with the most important addition of non-Markovian terms.

Usually, glasses can be analyzed with a fully classical approach since their transition temperatures are rather high. Nevertheless, in many cases of great interest the critical temperature can be lowered by tuning another external parameter and quantum fluctuations become very important. This is the case for the insulating magnetic compound  $\text{LiHo}_x\text{Y}_{1-x}\text{F}_4$ , that is an experimental realization of a quantum spin-glass, and presently receives much attention [25]. Other examples where glassy properties in the presence of quantum fluctuations have been observed are mixed hydrogen bonded ferro-antiferro electric crystals [26], interacting electron systems [27], cuprates like  $\text{La}_{2-x}\text{Sr}_x\text{CuO}_4$  [28], amorphous insulators [29], etc.

The quantum fluctuations in  $\text{LiHo}_x\text{Y}_{1-x}\text{F}_4$  can be controlled by tuning the strength of an external field that is transverse to the preferred direction of the randomly located magnetic impurities. After a series of experiments presented in [25] the authors' conclusions are: (1) The samples undergo a paramagnetic to spin-glass transition in the  $(T, \Gamma)$  plane, where  $\Gamma \propto H_t^2$  and  $H_t$  is the strength of the transverse field. (2) The transition is of second order (in the thermodynamic sense) close to the classical critical point  $(T = T_c, \Gamma = 0)$  but crosses over to first order close to the quantum critical point  $(T = 0, \Gamma = \Gamma_c)$ . (3) The system undergoes out of equilibrium dynamics in the glassy phase as demonstrated by the fact that the dynamics strongly depends on the preparation of the sample for all subsequent times explored experimentally.

The theoretical study of quantum spin-glasses started with Bray and Moore's analysis of the equilibrium properties of the fully connected Heisenberg model [30]. In this article, Bray and Moore introduced a path-integral representation in imaginary time of the partition function that they analyzed with the replica trick. Many articles on the equilibrium of this, and related, mean-field models have been published since [31, 32, 33, 34, 35, 36, 37, 38, 39]. The static properties of low dimensional models have been studied and it has been shown that, in finite dimensions, Griffiths-McCoy singularities are very important close to the quantum critical point [40]. In all these models, the transition from the paramagnetic to the spin-glass phase has been reported to be of second order throughout.

In most classical disordered models studied so far the transition from the disordered to the ordered phase is of second order in the thermodynamic sense. In the exact solution of the SK model, the spin-glass order parameter  $q(x)$  is continuous at the transition which is of second order in the thermodynamic sense [8]. In other classical glassy models like the Potts glass [9] or the spherical [41] and Ising [42, 43]  $p$  spin-glasses, the order parameter jumps at the transition which, however, is still of second-order in the thermodynamic sense since there is neither a jump in the susceptibility nor a latent heat. A classical model

that exhibits a first-order transition is the anisotropic  $p$  spin-glass,  $p \geq 3$ , in which the spins take integer values between  $-S$  and  $S$  and there is an extra term in the Hamiltonian  $-D \sum_i s_i^2$ , proportional to a coupling constant  $D$ , that controls the crystalline tendency. In this case, a crossover from a second-order to a first-order thermodynamic transition in the plane  $(T/J, D/J)$  has been exhibited in the exact solution [44]. The classical Ghatak-Sherrington (GS) model [15] is another candidate to exhibit a second to first order crossover in the thermodynamic transition. It is the anisotropic extension of the SK model, or the  $p = 2$  limit of the previous model. In this case, a crossover from a second order to a first order transition in the plane  $(T/J, D/J)$  has been exhibited in an *approximate* solution (one step replica symmetry breaking) [15, 16]. The exact solution has not been derived yet and it is then not well established if it has a true first-order thermodynamic transition.

In quantum problems, first order transitions have been reported in three models. The first one is the so-called “fermionic Ising spin-glass” analyzed by Oppermann and collaborators [45]. This model, however, is thermodynamically equivalent to the classical GS model discussed above [46]. The other two models are very similar indeed and they are different ways of extending the classical spherical  $p$  spin-glass model [41] to include quantum fluctuations. In one case, the continuous spins are generalized to  $M$  component vectors and a global spherical constraint as well as commutation relations are imposed [36]. The other one uses the fact that the spherical  $p$  spin-glass model can be interpreted as a particle moving in an infinite dimensional hyper-sphere with a random potential. Quantization is then done by imposing commutation relations between coordinates and momenta [37, 38]. The latter can also be interpreted as an extension of the a quantum rotor model [33] that includes  $p$  interactions. The relation between the critical properties of the quantum versions of  $p$  spin-glass models and the experiments in [25] has been put forward in [38]. In addition, the connection between the static calculation supplemented by the marginality condition and the analysis of the out of equilibrium dynamics in contact with an environment developed in [37] was also discussed in [38]. However, the reason why the transition changes from second to first order close to the quantum critical point was not clear from this analysis. It is one of the aims of this article to clarify this point, and study to what extent one can claim it to be general, with the use of the TAP approach.

Quantum TAP equations for the SK model in a transverse field have been presented by Ishii and Yamamoto [32] and Cesare *et al* [35]. The former use a perturbative expansion of the free-energy in the strength of the transverse field, and then follow closely TAP’s techniques; the latter implement a cavity method. The TAP equations derived by Rehker and Oppermann [18] for the fermionic spin-glass model coincide with the ones presented by Yokota [17] for the classical GS model since these two models are thermodynamically equivalent [46].

Hence, our aim is twofold. On the one hand we want to present a quantum extension of the TAP approach to the statistical properties of disordered systems. Thus, after a short revision of the classical TAP approach in Section 2, we discuss in Section 3 the derivation of the quantum TAP free-energy and TAP equations using a general approach that extends the ones developed by Plefka [5] and Georges and Yedidia [6]. The advantage with respect to previous derivations of quantum TAP equations is that this method can be applied to any quantum disordered model and it allows to obtain the TAP equations

as well as the TAP free energy. In Section 4 we present, as an example, the TAP free-energy and TAP-equations for the quantum extension of the  $p$  spin spherical spin-glass model studied in [38, 37]. We show that the TAP equations can be easily related to the equations for the order parameter in the Matsubara replica approach and also to some of the equations appearing in the real-time dynamic approach. The TAP analysis of this model furnishes a benchmark to study the generalization to the quantum case of the methods and interpretations developed for classical systems. Section 5 is devoted to the second aim of this article. Via the TAP approach we show that the same type of phase diagram naturally emerges for all systems having a discontinuous phase transition in their classical limit (these are models solved by a one-step replica symmetry breaking Ansatz within the replica analysis). In particular we relate the first-order transition close to the quantum critical point to the structure of metastable states. Finally, we present our conclusions in Section 6.

## 2 The classical TAP equations: a short revision

In this section we present a short revision of the classical TAP approach to mean-field disordered spin models. The classical TAP free-energy [1] is the Legendre transform of the free-energy with respect to local magnetic fields,

$$-\beta F(\beta, m_i) = \text{Tr} \exp \left( -\beta H - \sum_i h_i (s_i - m_i) \right) , \quad (1)$$

where  $h_i$  are Lagrange parameters enforcing the condition  $\langle s_i \rangle = m_i$ .  $-\beta F(\beta, m_i)$  is an effective potential that depends on the local magnetizations. The Lagrange conditions  $-\partial \beta F / \partial m_i = h_i$ , called TAP equations, fix the local magnetizations as functions of the local magnetic fields <sup>1</sup>. The solutions  $\{m_i^\alpha\}$  of the TAP equations are stationary points of  $F(\beta, m_i)$ . If they are also stable (all the corresponding eigenvalues of the free-energy Hessian are positive), they are identified [8] with pure states, also called TAP states. This interpretation was put forward by De Dominicis and Young [7] who showed that the partition function in the classical SK model can be written as a weighted sum over the stable solutions of the TAP equations:

$$Z = \sum_\alpha \exp(-\beta F(\beta, \mathbf{m}^\alpha)) , \quad (2)$$

where the index  $\alpha$  labels different TAP states,  $\mathbf{m}^\alpha$  is an  $N$ -vector encoding the local magnetization in the solution  $\alpha$ ,  $F$  is the extensive TAP free-energy of such solution and the sum runs over all TAP solutions. Consequently, the static average of any observable can be computed from Eq. (2). At low temperatures the TAP free-energy has a large number of minima. If one groups different TAP states with the same free-energy in sets  $\mathcal{C}$  then the partition function can be written as

$$Z = \sum_{\mathcal{C}} \mathcal{N}(f, \beta) \exp(-\beta N f) \quad (3)$$

---

<sup>1</sup>Note that within the TAP approach one does not average over disorder from the beginning as in the replica method. Consequently the TAP free energy depends on the particular realization of disorder.

where the factor  $\mathcal{N}(\beta, f)$  is the number of solutions with TAP free-energy density  $F(\beta, \mathbf{m}^\alpha)/N = f$ . One can now replace the sum by an integral and exponentiate the factor  $\mathcal{N}(\beta, f)$ ; this yields

$$\lim_{N \rightarrow \infty} \frac{1}{N} \ln Z = \lim_{N \rightarrow \infty} \frac{1}{N} \ln \int df \exp(-N(\beta f - \sigma(\beta, f))) \quad (4)$$

where we have taken the continuous limit and introduced the *complexity*

$$\sigma(\beta, f) \equiv \lim_{N \rightarrow \infty} \frac{1}{N} \ln (\mathcal{N}(\beta, f)) . \quad (5)$$

The configurations that dominate the sum are those having a free-energy density such that it minimizes  $\beta f - \sigma(\beta, f)$ . The identity between the partition function and the weighted sum over TAP solutions has been demonstrated for many others models [12, 9, 47] and it is generally believed to hold for any mean-field disordered system.

In the following we focus on “discontinuous glassy systems” [20] that are characterized by having a discontinuous transition (the Edwards-Anderson order parameter,  $q_{\text{EA}}$ , jumps) that is still of second order thermodynamically. Within the replica analysis of the partition function these models are characterized by a one-step replica symmetry breaking solution below a static transition temperature  $T_s$  and a replica symmetric (RS) solution, that corresponds to the paramagnetic phase, at  $T > T_s$ . However, for intermediate temperatures  $T_s < T < T_d$  there are an exponential in  $N$  number of non-trivial TAP solutions that combine themselves in such a way that the sum (4) is identical to the RS result.

The relationship between metastable states and replicas has been put forward in [43, 47, 49]. Indeed, consider  $x$  different identical systems (“clones”) coupled by an attractive, infinitesimal (but extensive) interaction. When there exist many pure states all the clones fall into the same state and the free energy for the system of  $x$  clones reads:

$$\lim_{N \rightarrow \infty} \frac{-1}{\beta N} \ln Z_x = \lim_{N \rightarrow \infty} \frac{-1}{\beta N} \ln \int df \exp(-N(\beta x f - \sigma(\beta, f))) . \quad (6)$$

On the other hand the computation of the left hand-side of (6) can be performed within the replica formalism:

$$\lim_{N \rightarrow \infty} \frac{-1}{\beta N} \ln Z_x = \lim_{N \rightarrow \infty} \frac{-1}{\beta N} \overline{\ln Z_x} = \lim_{N \rightarrow \infty, n \rightarrow 0} \frac{-1}{\beta N n} \ln \overline{Z_x^n} \quad (7)$$

where the overline represents the average over disorder. Since the attractive coupling between the  $x$  clones is infinitesimal, the computation of the right-hand side of (7) reduces simply to the calculation of  $\lim_{n' \rightarrow 0} (x/n') \ln \overline{Z^{n'}}$ , where the replica symmetry between the  $n$  groups of  $x$ -replicas ( $n' = nx$ ) is *explicitly* broken. When the system is in the replica symmetric phase ( $T_s < T$ ), this reduces to study one-step solutions non-optimized with respect to  $x$ :

$$-\lim_{N \rightarrow \infty} \frac{1}{\beta N} \ln \int df \exp(-N(\beta x f - \sigma(\beta, f))) = x \text{Extr}_{q_{\text{EA}}} f_{\text{REP}}(q_{\text{EA}}; \beta, x) \quad (8)$$

where  $f_{\text{REP}}$  is the free-energy computed by using replicas,  $q_{\text{EA}}$  is the Edwards-Anderson parameter and  $x$  is the breakpoint (or the size of the blocks in the replica matrix). For

simplicity we consider that the inter-state overlap  $q_0$  equals zero. The definitions of these parameters are standard in the replica approach [8] and they will appear in the analysis of the quantum  $p$  spin-glass model in Section 3. Since the integral on the left-hand-side of (8) is dominated by a saddle point contribution, one finds that, for a given temperature, fixing the value of  $x$  is equivalent to summing over states with a given energy density  $f$ . The relationship between  $f$  and  $x$  reads

$$\beta x = \frac{\partial \sigma(\beta, f)}{\partial f} . \quad (9)$$

Note that within this framework one does not have to optimize with respect to  $x$ . Instead,  $x$  is a free parameter and, by changing the value of  $x$ , one can consider different groups of metastable states.

The analysis of the TAP equations reveals three temperature regimes for discontinuous glassy systems:

- *High temperatures*  $T_d < T$ . The system is in the paramagnetic phase, the paramagnetic TAP solution  $m_i = 0$ , for all  $i$ , dominates the sum and  $f_{pm} = -\ln Z/(\beta N)$ .  $T_d$  is the dynamic critical temperature. Above  $T_d$  the dynamics starting from a random initial condition converges asymptotically to the paramagnetic solution.
- *Intermediate temperatures*  $T_s < T < T_d$ . The replica analysis of the partition function indicates that the system is still in the paramagnetic phase. However, the study of the TAP equations and the dynamics show that at  $T_d$  the paramagnetic solution is fractured in an exponentially large in  $N$  number of minima of the TAP free-energy [11, 9, 48, 49]. Indeed one can recover these results also by the replica method. A careful replica analysis shows that there exist one-step solutions in these temperature regime other than the paramagnetic one. These solutions are in one to one correspondence with groups of states with a given free-energy density (through the relationship (9)). For instance, one can follow the evolution of the threshold states (the states with highest free-energy) by tuning the parameter  $x$ . For these states,  $x = 1$  when  $T = T_d$  and decreases at lower temperatures. Moreover, the dominant contribution to Eq. (4) is given by the states characterized by  $x = 1$ , *i.e.* those with free-energy density such that

$$\beta = \frac{\partial \sigma(\beta, f)}{\partial f} . \quad (10)$$

These are the threshold states at  $T_d$  and other groups when  $T < T_d$ . Hence, between  $T_s < T < T_d$  saddle-point solutions (corresponding to  $x = 1$ ) that are not absolute minima of  $F$  dominate the integral since their number scales exponentially with  $N$ . The final result for the free-energy density in this temperature range coincides with the one of the prolongation of the paramagnetic solution (that actually does not exist!). A naive replica computation fails to signal the difference between a true paramagnetic solution and the ensemble of non trivial TAP solutions with  $m_i \neq 0$ . The dynamic approach detects the change in free-energy landscape at  $T_d$  since the system cannot reach equilibrium for any temperature below  $T_d$  [22].

- *Low temperatures*  $T < T_s$ . At the static transition temperature the complexity of the TAP solutions, which dominates the sum (4), vanishes. The static transition appears as an *entropy crisis* since the part of the total entropy that is related to the large number of states disappears. For  $T < T_s$  the TAP states which dominate the integral in Eq. (4) correspond to the equilibrium glassy phase. Dynamically,  $T_s$  does not play any role. The out of equilibrium dynamics is dominated by the threshold states, which are the highest ones in free-energy and that are characterized by flat directions in the free-energy landscape.

Note that via the TAP approach one can obtain a reasonable justification of the marginality condition [50] often used to obtain information about the out of equilibrium dynamics starting from a pure equilibrium computation [51]. Indeed the value of  $x$  fixed by the marginality condition corresponds to the TAP states which are marginally stable (the threshold states): the flatness of the free-energy landscape around these states is responsible for aging [22].

### 3 The quantum TAP equations

In this section we present a simple procedure to derive TAP equations for generic completely connected quantum systems. We also expose the physical meaning of quantum TAP equations by the cavity method [8].

We are aware of two publications where TAP equations for quantum systems have been already presented [32, 35]. With respect to these works our derivation is more systematic, simple and it allows one to obtain the TAP equations as well as the TAP free-energy for any completely connected quantum disordered system.

#### 3.1 Formalism, notations and models

The formalism that we use to derive TAP equations for generic quantum problems is very similar to the one described in [5, 6] and, it follows even more closely, the one used in [24] to obtain the dynamical TAP equations for classical disordered models.

We focus on systems characterized by the potential energy:

$$H_p = - \sum_{i_1 < \dots < i_p} \sum_{\alpha} J_{i_1, \dots, i_p} s_{i_1}^{\alpha} \cdots s_{i_p}^{\alpha} \quad i = 1, \dots, N \quad \alpha = 1, \dots, m \quad (11)$$

where  $\mathbf{s}_i$  may represent an SU(2) spin ( $m = 3$ ), a rotor ( $m > 1$ ), a spherical spin ( $m = 1$ ) or a space-coordinate ( $m = 1$ ) and  $J_{i_1, \dots, i_p}$ , the couplings between the different  $\mathbf{s}_i$ , are independent random variables with zero mean and variance

$$\overline{(J_{i_1 \dots i_p})^2} = \frac{\tilde{J}^2 p!}{2N^{p-1}}. \quad (12)$$

As a consequence the following derivation applies to (completely connected) Heisenberg models, quantum rotor models and quantum continuous systems<sup>2</sup>. Without loss of gen-

---

<sup>2</sup> The results obtained in this section can be straightforwardly generalized to more complicate potentials containing different monomials or characterized by a more complicate tensorial coupling between  $s_{i_1}^{\alpha_1}, \dots, s_{i_p}^{\alpha_p}$ .

erality and to simplify the notation we shall suppress the index  $\alpha$  in the rest of this section.

For classical spin-glasses TAP showed that all the local magnetizations  $m_i$ ,  $i = 1, \dots, N$ , are needed to derive the relevant free-energy density to describe the metastable properties [1]. If one is interested in the dynamics of classical disordered mean-field systems, one has to Legendre transform not only with respect to all time-dependent local magnetizations  $m_i(t)$ , but also with respect to the autocorrelation  $C(t, t') = 1/N \sum_i \langle s_i(t) s_i(t') \rangle$  and the linear response  $R(t, t') = 1/N \sum_i \delta \langle s_i(t) \rangle / \delta h_i(t')|_{h=0}$  [24].

In order to describe the metastable properties of a quantum disordered model we shall show that it is necessary to Legendre transform with respect to the local average coordinates,  $m_i(\tau)$ , and the autocorrelation function in imaginary time,  $C(\tau, \tau')$ . The quantum TAP free-energy reads

$$\begin{aligned} -\beta F(\beta, m_i(\tau), C(\tau, \tau'), \alpha)|_{\alpha=1} = & \ln \int \mathcal{D}\mathbf{s}(\tau) \exp \left[ -\frac{1}{\hbar} \int_0^{\beta\hbar} d\tau (H_k + \alpha H_p(\mathbf{s})) \right. \\ & + \frac{1}{2\hbar^2} \int_0^{\beta\hbar} d\tau \int_0^{\beta\hbar} d\tau' \sum_i \Lambda(\tau, \tau') (C(\tau, \tau') - s_i(\tau) s_i(\tau')) \\ & \left. + \frac{1}{\hbar} \int_0^{\beta\hbar} d\tau \sum_i h_i(\tau) (m_i(\tau) - s_i(\tau)) \right] \Big|_{\alpha=1}. \end{aligned} \quad (13)$$

where  $H_k$  is the kinetic energy,  $\mathcal{D}\mathbf{s}(\tau)$  indicates the functional measure on the configuration space and  $\alpha$  is a parameter whose role will be clarified in the following. For instance, if  $\mathbf{s}_i$  are SU(2) spins  $H_k$  is the Berry phase and the functional measure is restricted to periodic functions  $\mathbf{s}_i(\tau)$  (with period  $\beta$ ) satisfying the constraint  $\mathbf{s}_i^2(\tau) = 1$ . The sources  $h_i(\tau)$  and  $\Lambda(\tau, \tau')$  have the role of Lagrange multipliers fixing the average value of the coordinates and the correlation:

$$m_i(\tau) = \langle s_i(\tau) \rangle, \quad (14)$$

$$C(\tau, \tau') = \frac{1}{N} \sum_i \langle s_i(\tau) s_i(\tau') \rangle. \quad (15)$$

Once the TAP free-energy  $F$  is known, one can derive the TAP equations as Legendre relations,

$$-\frac{\delta \beta F}{\delta m_i(\tau)} = h_i(\tau), \quad -\frac{2}{N} \frac{\delta \beta F}{\delta C(\tau, \tau')} = \Lambda(\tau, \tau'). \quad (16)$$

Until now we have not used the scaling (12) and all these definitions can be equally applied to finite dimensional systems. The great simplification due to the mean field character of the interactions in (12) is unveiled if one performs a perturbative expansion of Eq. (13) in  $\alpha$  and writes  $-\beta F(\beta, m_i(\tau), C(\tau, \tau'), \alpha)$  as a power series in  $\alpha$ :

$$-\beta F(\beta, m_i(\tau), C(\tau, \tau'), \alpha) = \sum_{n=0}^{\infty} \frac{1}{n!} \frac{\partial^n (-\beta F(\beta, m_i(\tau), C(\tau, \tau'), \alpha))}{\partial \alpha^n} \Big|_{\alpha=0} \alpha^n. \quad (17)$$

In fully-connected models, if one chooses the correct order parameters (which are  $m_i(\tau)$ ,  $C(\tau, \tau')$  in the quantum case), the perturbative expansion (17) around the pure kinetic

theory is actually a simple sum over three terms. Higher order terms in the series vanish in the thermodynamic limit due to the scaling of  $J_{i_1, \dots, i_p}$  with respect to  $N$ . In more general cases, in finite dimensions, this will not be the case and (17) becomes a  $1/d$  expansion around mean field theory, where  $d$  is the spatial dimension [6].

Let us consider in more detail the terms arising from the expansion (17). The zeroth-order one is simply  $-\beta F(\beta, m_i(\tau), C(\tau, \tau'), 0)$ , i.e. the free-energy of  $N$  free spins constrained to have local magnetizations  $m_i(\tau)$  and a global correlation function  $C(\tau, \tau')$ . This term depends only on the nature of the degrees of freedom, whether they are  $SU(2)$  spins, rotors or space-coordinates. In particular it can be analytically computed only if  $s_i$  are spherical spins or space-coordinates. In the other cases one has to resort to approximations or numerical computations.

The first-order term is the naive mean field free-energy:

$$\frac{\partial(-\beta F)}{\partial \alpha} \Big|_{\alpha=0} = \frac{1}{\hbar} \int_0^{\beta \hbar} \sum_{i_1 < \dots < i_p} J_{i_1, \dots, i_p} \langle s_{i_1} \cdots s_{i_p} \rangle_{\alpha=0} = \frac{1}{\hbar} \int_0^{\beta \hbar} \sum_{i_1 < \dots < i_p} J_{i_1, \dots, i_p} m_{i_1} \cdots m_{i_p}. \quad (18)$$

Note that the decoupling of the spins for  $\alpha = 0$  is essential to obtain the last identity. The second-order term depends on the correlation function and the overlap function  $Q(\tau, \tau') = \sum_i m_i(\tau) m_i(\tau')/N$  only and equals

$$\frac{N \tilde{J}^2}{4\hbar^2} \int_0^{\beta \hbar} d\tau \int_0^{\beta \hbar} d\tau' \left( C^p(\tau, \tau') - Q^p(\tau, \tau') - p(C(\tau, \tau') - Q(\tau, \tau')) Q^{p-1}(\tau, \tau') \right), \quad (19)$$

Using the scaling of the couplings with  $N$  and by the same arguments developed for classical systems [5, 12], we have verified that all orders  $n \geq 3$  in the series (17) are suppressed in the thermodynamic limit.

### 3.2 A cavity interpretation

First of all, let us write the TAP equations in a way which allows one to clarify the physical meaning of the different terms:

$$\begin{aligned} \frac{\delta(-\beta F)}{\delta m_i(\tau)} \Big|_{\alpha=0} &= h_i^{cav}(\tau) = - \sum_{i_2 < \dots < i_p} J_{i, i_2, \dots, i_p} m_{i_2}(\tau) \dots m_{i_p}(\tau) \\ &\quad - \frac{1}{\hbar} \int_0^{\beta \hbar} d\tau' \left[ \frac{p(p-1)}{2} (Q(\tau, \tau') - C(\tau, \tau')) Q^{p-2}(\tau, \tau') \right] m_i(\tau'), \end{aligned} \quad (20)$$

$$\frac{2}{N} \frac{\delta(-\beta F)}{\delta C(\tau, \tau')} \Big|_{\alpha=0} = G^{cav}(\tau, \tau') = \frac{p}{2} [Q^{p-1}(\tau, \tau') - C^{p-1}(\tau, \tau')]. \quad (21)$$

The solutions to these equations are expected to be time-translation invariant since we are developing a description of equilibrium and metastable properties. Therefore  $h_i^{cav}$  is indeed independent of the imaginary time and  $G^{cav}$  depends only on the difference between  $\tau$  and  $\tau'$ .

An understanding of the meaning of the quantum TAP equations follows from the analysis of  $F$  for  $\alpha = 0$ . Indeed, by tracing out all the spins except  $s_i$  in the partition

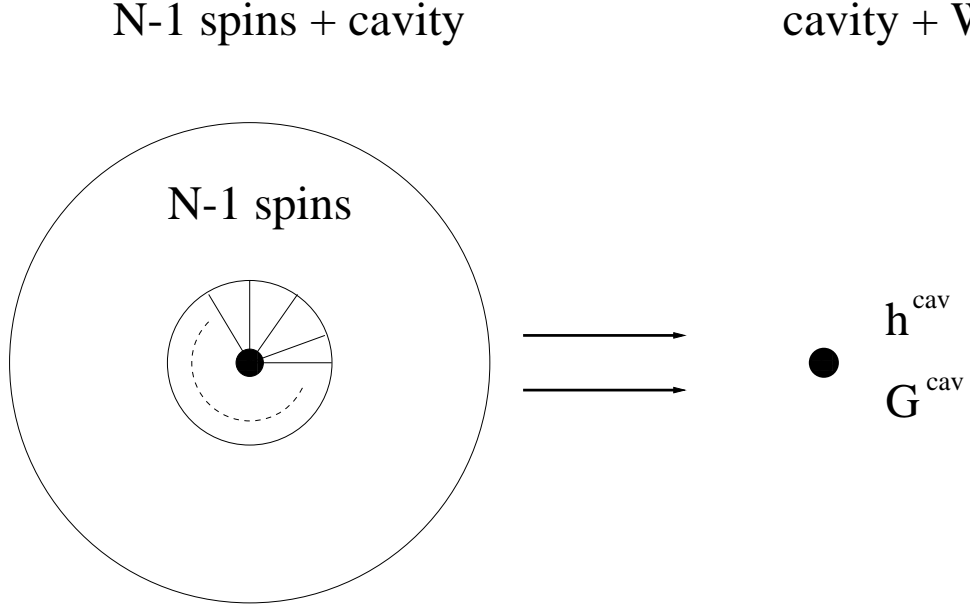


Figure 1: A schematic representation of the action of the  $N - 1$  spins on the cavity which, due to the infinite connectivity, simply reduces to  $h_i^{cav}$  and  $G^{cav}$ .

function produces a single-site measure (for  $s_i$ ) whose action reads:

$$-\frac{1}{\hbar} \int_0^{\beta\hbar} d\tau [H_k(s_i(\tau)) + h_i^{cav}(\tau)s_i(\tau)] - \frac{1}{2\hbar^2} \int_0^{\beta\hbar} d\tau \int_0^{\beta\hbar} d\tau' s_i(\tau) G^{cav}(\tau, \tau') s_i(\tau') , \quad (22)$$

where  $H_k(s_i(\tau))$  is the kinetic energy for the spin  $s_i$ . As a consequence the TAP solutions are the self-consistent relations that relate  $G^{cav}(\tau, \tau')$  and  $h_i^{cav}(\tau)$  (which are functions of  $C(\tau, \tau')$  and  $m_i(\tau)$ ) to  $C(\tau, \tau')$  and  $m_i(\tau)$  obtained from the single-site action (22).

Equations (20) and (21) show that the action on the  $i$ th spin of the  $N - 1$  remaining ones reduces simply to  $h_i^{cav}$  and  $G^{cav}$ . This implies that tracing out all the spins but the  $i$ th one produces a Gaussian measure for the instantaneous magnetic fields  $h_i(\tau) = -\sum_{i_2 < \dots < i_p} J_{i_1, \dots, i_p} s_{i_1} \cdots s_{i_p}$ , whose mean and connected two-point correlation function equal respectively  $h_i^{cav}$  and  $G^{cav}(\tau - \tau')$ .

The expression of  $h_i^{cav}$  and  $G^{cav}(\tau - \tau')$  can be justified within the cavity method [8]. Let us focus for simplicity on the  $p = 2$  case for which

$$h_i^{cav} = - \sum_k J_{i,k} \langle s_k \rangle_{N-1} \quad (23)$$

where  $\langle \cdot \rangle_{N-1}$  represents the thermal average with respect to the system with the  $i$ th site removed.  $\langle s_k \rangle_{N-1}$  is not simply equal to  $m_k$ , which is the mean magnetization for the system of  $N$  spins. A correction term, first discovered by Onsager, appears:

$$\langle s_k \rangle_{N-1} = m_k - \frac{1}{\hbar} \int_0^{\beta\hbar} d\tau \frac{\delta m_k(\tau)}{h_k(\tau')} J_{i,k} m_i(\tau') = m_k - \frac{1}{\hbar} \int_0^{\beta\hbar} d\tau [C(\tau) - Q] J_{i,k} m_i \quad (24)$$

Plugging Eq. (24) into Eq. (23) and using the scaling of the couplings with  $N$  one recovers

the expression for  $h_i^{cav}$  given in (20) in the  $p = 2$  case. Whereas for  $G^{cav}$  a similar computation<sup>3</sup> gives back the expression given in (21).

Finally, we remark that the main difference between the classical and the quantum TAP approach is that in the latter the cavity interaction consists not only in a cavity field but also in the “Weiss function”  $G^{cav}(\tau - \tau')$ , which is a function of (imaginary) time. This already happens in the mean-field theory of quantum non-disordered systems [52] for which local quantum fluctuations are taken into account exactly, whereas the spatial ones are frozen. For disordered systems, even in the limit of infinite dimensions, one has to take into account not only the local quantum fluctuations but also some spatial fluctuations: all the instantaneous magnetic fields have the same variance but their averaged values fluctuate from site to site.

## 4 A continuous disordered quantum model

In this Section we apply the method of Section 3 to the study of the quantum spherical  $p$  spin-glass model. We derive and analyze the TAP free-energy density and the TAP equations for the local magnetization and correlation function in imaginary time. We relate these equations to the equation for the order parameter in the Matsubara replicated approach to equilibrium and in the Schwinger-Keldysh approach to the non-equilibrium dynamics.

### 4.1 The model and its TAP equations

A model of a quantum particle with position  $\mathbf{s}$  and momentum  $\mathbf{p}$  that moves on an  $N$ -dimensional random environment is defined as

$$H[\mathbf{p}, \mathbf{s}, J] = \frac{\mathbf{p}^2}{2M} - \sum_{i_1 < \dots < i_p}^N J_{i_1 \dots i_p} s_{i_1} \dots s_{i_p} . \quad (25)$$

A Lagrange multiplier  $z$  enforces the averaged spherical constraint

$$\frac{1}{N} \sum_{i=1}^N \langle s_i^2 \rangle = 1 . \quad (26)$$

The random interaction strengths  $J_{i_1 \dots i_p}$  are taken with zero mean and variance defined in Eq. (12). This model is a possible quantum extension of the spherical  $p$  spin-glass model introduced in [41] and it is a particular realization of the class defined in (11) corresponding to space-coordinates  $s_i$  constrained to move on a  $N$ -dimensional sphere.

The zero-th order term of the expansion (17) can be readily computed for this model. By setting  $\alpha = 1$ , rescaling time according to  $\tau \rightarrow \tau\hbar/\tilde{J}$ , and defining the “quantum parameter”  $\Gamma \equiv \hbar^2/(\tilde{J}M)$  we obtain the following expression for the quantum TAP free-energy (13) :

$$-\beta F = \frac{N}{2} \text{Tr} \ln(C - Q) + \frac{N}{2\Gamma} \text{Tr} \left( \frac{\partial^2 C}{\partial \tau^2} \right) + \int_0^\beta d\tau \sum_{i_1 < \dots < i_p} J_{i_1 \dots i_p} m_{i_1}(\tau) \dots m_{i_p}(\tau)$$

---

<sup>3</sup>Indeed easier since there is no reaction term for  $G^{cav}$  on a completely connected lattice.

$$\begin{aligned}
& + \frac{N}{4} \int_0^\beta d\tau \int_0^\beta d\tau' \left( C^p(\tau, \tau') - Q^p(\tau, \tau') - p(C(\tau, \tau') - Q(\tau, \tau')) Q^{p-1}(\tau, \tau') \right) \\
& - \frac{N\beta}{2} \int_0^\beta d\tau z(\tau) (C(\tau, \tau) - 1)
\end{aligned} \tag{27}$$

The physical parameters  $m_i(\tau)$  and  $C(\tau, \tau')$  are fixed by the quantum TAP equations (16)

$$\begin{aligned}
h_i(\tau) &= \sum_{i_2 < \dots < i_p} J_{i, i_2, \dots, i_p} m_{i_2}(\tau) \dots m_{i_p}(\tau) \\
& + \int_0^\beta d\tau' \left[ -(C - Q)^{-1}(\tau, \tau') + \frac{p(p-1)}{2} (Q(\tau, \tau') - C(\tau, \tau')) Q^{p-2}(\tau, \tau') \right] m_i(\tau') , \\
z(\tau) \delta(\tau - \tau') &= (C - Q)^{-1}(\tau, \tau') + \delta(\tau - \tau') \frac{1}{\Gamma} \frac{\partial^2}{\partial \tau^2} + \frac{p}{2} [C^{p-1}(\tau, \tau') - Q^{p-1}(\tau, \tau')] .
\end{aligned} \tag{28}$$

Finally, setting  $h_i(\tau) = 0$  and using that at stationarity,  $m_i(\tau) = m_i$ ,  $Q(\tau, \tau') = q_{\text{EA}}$ ,  $z(\tau) = z$  and  $C(\tau, \tau') = C(\tau - \tau')$ , the previous equations are simplified to

$$\begin{aligned}
\frac{1}{\Gamma} \frac{\partial^2 C(\tau)}{\partial \tau^2} &= -\frac{p}{2} \int_0^\beta d\tau' (C^{p-1}(\tau - \tau') - q_{\text{EA}}^{p-1}) (C(\tau') - q_{\text{EA}}) \\
& + z(C(\tau) - q_{\text{EA}}) - \delta(\tau) ,
\end{aligned} \tag{29}$$

$$\begin{aligned}
zm_i &= \sum_{i_2 < \dots < i_p} J_{i, i_2, \dots, i_p} m_{i_2} \dots m_{i_p} + \\
& m_i \frac{p}{2} \int_0^\beta d\tau' \left( C^{p-1}(\tau') + (p-2)q_{\text{EA}}^{p-1} - (p-1)C(\tau')q_{\text{EA}}^{p-2} \right) .
\end{aligned} \tag{30}$$

## 4.2 Analysis of the quantum TAP equations

In the classical case the TAP equations admit a large number of solutions at low temperatures. In the following we shall show that this remains the case in a certain regime of  $T$  and  $\Gamma$ . Furthermore we shall classify them by their Edwards-Anderson parameters. Finally, we shall exhibit several properties of the TAP solutions valid at low temperatures.

### 4.2.1 A simple equation on the Edwards-Anderson parameter

Let us analyze in detail the equations for the local magnetizations,  $m_i$ . First of all we note that a simple equation that relates  $q_{\text{EA}}$  to the potential energy density derives from Eq. (28). In fact, by multiplying Eq. (28) by  $m_i/N$  and summing over  $i = 1, \dots, N$  one obtains (for  $h_i = 0$ )

$$0 = -\frac{q_{\text{EA}}}{\tilde{C}(0) - \beta q_{\text{EA}}} + \frac{p}{N} \sum_{i_1 < \dots < i_p} J_{i_1 \dots i_p} m_{i_1} \dots m_{i_p} - \frac{p(p-1)}{2} (\tilde{C}(0) - \beta q_{\text{EA}}) q_{\text{EA}}^{p-1} \tag{31}$$

where we introduced the discrete Fourier transform of the correlation

$$\tilde{C}(\omega) \equiv \int_0^\beta d\tau e^{i\omega\tau} C(\tau) . \tag{32}$$

Following Kurchan *et al* [11], we introduce the *angular* variables  $\sigma_i = m_i / \sqrt{q_{\text{EA}}}$  and define the *angular potential energy density*

$$\mathcal{E}(\sigma) \equiv -\frac{1}{N} \sum_{i_1 < \dots < i_p} J_{i_1 \dots i_p} \sigma_{i_1} \dots \sigma_{i_p}. \quad (33)$$

For any fixed energy level  $\mathcal{E}$ , Eq. (31) becomes a second-order polynomial equation for  $q_{\text{EA}}$ ; the solution is determined by

$$q_{\text{EA}}^{p/2-1}(\tilde{C}(0) - \beta q_{\text{EA}}) = z_{\pm} = \frac{1}{p-1} \left( -\mathcal{E}(\sigma) \pm \sqrt{\mathcal{E}^2(\sigma) - \mathcal{E}_{\text{TH}}^2} \right) \quad (34)$$

and  $\mathcal{E}_{\text{TH}}$ , called the threshold value, is given by

$$\mathcal{E}_{\text{TH}} = -\sqrt{\frac{2(p-1)}{p}}. \quad (35)$$

The right-hand-side of Eq. (34) has to be real. This imposes the condition  $\mathcal{E} \leq \mathcal{E}_{\text{TH}}$  since  $\mathcal{E}$  is a negative quantity.

For each sign in Eq. (34), its left-hand-side has a bell-shape as a function of  $q_{\text{EA}}$ . It vanishes at  $q_{\text{EA}} = 0$  and  $q_{\text{EA}} = \tilde{C}(0)/\beta$  and attains its maximum at  $q_{\text{EA}} = (1-2/p)\tilde{C}(0)/\beta$ . Hence, at fixed values of  $\mathcal{E}$  and  $T$ , Eq. (34) has none or *two* solutions,  $q_{\text{EA}} = q', q''$ , with

$$0 \leq q' \leq \frac{(1-2/p)\tilde{C}(0)}{\beta}, \quad (36)$$

$$\frac{(1-2/p)\tilde{C}(0)}{\beta} \leq q'' \leq \frac{\tilde{C}(0)}{\beta} \quad (37)$$

(we assume, as expected, that  $C(\tau)$  is positive for all  $\tau$ ). In the classical case, the minus sign in Eq. (34) leads to a value of  $q_{\text{EA}}$  that is a minimum of the TAP free-energy for all  $\mathcal{E} < \mathcal{E}_{\text{TH}}$ . The Edwards-Anderson parameter determined in this way has the expected physical behavior [12]. In Appendix A we show that in the quantum case one has to choose the minus sign in Eq. (34), too. Thus,  $q_{\text{EA}}$  is determined by

$$q_{\text{EA}}^{p/2-1}(\tilde{C}(0) - \beta q_{\text{EA}}) = \frac{1}{p-1} \left( -\mathcal{E}(\sigma) - \sqrt{\mathcal{E}^2(\sigma) - \mathcal{E}_{\text{TH}}^2} \right). \quad (38)$$

This equation still has two solutions. It can be proven that the solution with the larger absolute value of  $q_{\text{EA}}$  has the correct physical properties. In particular, it is connected to the classical solution, and it is then the solution to be kept. Thus there is a one to one correspondence between  $q_{\text{EA}}$  and  $\mathcal{E}$ .

It is of particular interest, as we shall show below, the *threshold solution*  $\mathcal{E} = \mathcal{E}_{\text{TH}}$ . In this case the equation for  $q_{\text{EA}}$  becomes

$$1 = \frac{p(p-1)}{2} (\tilde{C}(0) - \beta q_{\text{EA}})^2 q_{\text{EA}}^{p-2}. \quad (39)$$

Note that this equation coincides with the one found with the Matsubara formalism using the marginality condition to fix the block size  $x$  in the replica matrix [38]. Furthermore, it coincides with the equation for the dynamic value of the Edwards-Anderson

parameter  $q_{\text{EA}} \equiv \lim_{t \rightarrow \infty} \lim_{t_w \rightarrow \infty} C(t + t_w, t_w)$  obtained from the study of the real-time dynamics of the quantum model evolving in contact with an Ohmic quantum environment [37], when one takes first the thermodynamic limit, next the long-time limit of the system's dynamics in contact with the environment and, finally, the strength of the coupling to the environment to zero. The relationship between TAP, Matsubara and dynamical approach will be discussed in Section 4.3.

#### 4.2.2 Multiplicity of TAP solutions

The equations (34) reveal an interesting structure of the TAP equations (29) and (30). For a given value of the angular potential energy  $\mathcal{E}$  the TAP equations decouple in two different sets: Eqs. (29) and (34), with the spherical condition on  $C$ , determine the correlation function, the spherical parameter and the Edwards-Anderson parameter; whereas Eqs. (30) determine the angular variables only. They read

$$\mu q_{\text{EA}}^{1-p/2} \sigma_i = -p\mathcal{E}(\sigma)\sigma_i = p \sum_{i_2 < \dots < i_p} J_{i,i_2,\dots,i_p} \sigma_{i_2} \dots \sigma_{i_p}, \quad (40)$$

$$\mu \equiv z - \frac{p(p-2)\beta}{2} q_{\text{EA}}^{p-1} + \frac{p(p-1)}{2} \tilde{C}(0) q^{p-2} - \tilde{\Sigma}(0), \quad (41)$$

where we have defined

$$\tilde{\Sigma}(0) \equiv \frac{p}{2} \int_0^\beta C^{p-1}(\tau). \quad (42)$$

For a given value of the angular potential energy  $\mathcal{E}$  Eqs. (40) allow one to determine the angular part of the TAP solutions.

In general for a given value of  $\mathcal{E}$ , Eqs. (29) and (34) determine the correlation function, the spherical parameter and the Edwards-Anderson parameter *in a unique way*. (An exception to this rule are the paramagnetic solutions which however do not correspond to any  $\mathcal{E}$ .) As a consequence, the multiplicity of TAP solutions is entirely due to Eq. (40) which, for certain values of  $\mathcal{E}$ , can admit an exponential (in  $N$ ) number of solutions  $\mathcal{N}(\mathcal{E})$ . The complexity as a function of  $\mathcal{E}$  is then defined as

$$\sigma(\mathcal{E}) \equiv \lim_{N \rightarrow \infty} \frac{1}{N} \overline{\ln(\mathcal{N}(\mathcal{E}))}, \quad (43)$$

Equation (40) already appears at the classical level. The complexity has been computed by Crisanti and Sommers [12] and Cavagna *et al.* [13] with the following result. There are typically no solutions for  $\mathcal{E} < \mathcal{E}_{\text{EQ}}$ , whereas for  $\mathcal{E}_{\text{EQ}} < \mathcal{E} < \mathcal{E}_{\text{TH}}$  the complexity reads

$$\begin{aligned} \sigma(\mathcal{E}) = & \frac{1}{2} \left( 1 + \ln \left( \frac{p}{2} \right) \right) - \mathcal{E}^2 + \left( \frac{\mathcal{E} - \sqrt{\mathcal{E}^2 - \mathcal{E}_{\text{TH}}^2}}{\sqrt{2}\mathcal{E}_{\text{TH}}} \right)^2 + \ln \left( -\mathcal{E} - \sqrt{\mathcal{E}^2 - \mathcal{E}_{\text{TH}}^2} \right) \\ & \text{for } \mathcal{E}_{\text{EQ}} < \mathcal{E} < \mathcal{E}_{\text{TH}} \end{aligned} \quad (44)$$

where  $\mathcal{E}_{\text{EQ}}$  is the value at which  $\sigma(\mathcal{E})$  vanishes. A plot of this function is traced in Fig. 2 for  $p = 3$ .

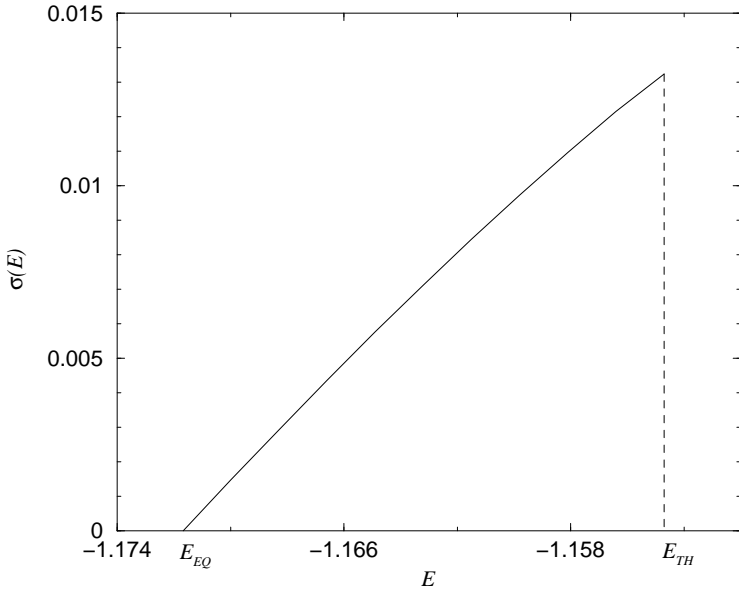


Figure 2: The complexity  $\sigma(\mathcal{E})$  as a function of  $\mathcal{E}$  in the interval  $\mathcal{E}_{\text{EQ}} < \mathcal{E} < \mathcal{E}_{\text{TH}}$  for  $p = 3$ .

#### 4.2.3 A low temperature and low $\Gamma$ approximation

In the classical case the TAP equations separate in two sets:  $N$  equations for the angular variables and one for the Edwards-Anderson parameter. The former admit an exponential number of solution and are studied from a statistical point of view (one computes the number of solution, and the typical properties of solution corresponding to a given  $\mathcal{E}$ ), whereas the latter can be easily solved. In the quantum case the analysis of the equations for the angular variables is identical to the one used for classical systems. The analog of the equation that determines  $q_{\text{EA}}$  becomes now a differential equation for  $C(\tau)$  that has to be studied numerically. This differential equation can be mapped exactly onto the ones analysed with the replica method, as we shall show in Section (4.3), and its numerical solution can be found in [38]. In this section we perform a low-temperature and low  $\Gamma$  approximation, also discussed in [38], that allows one to obtain some qualitative results that remain valid for the exact solution.

At low temperature and low  $\Gamma$ , the extension of the imaginary time-interval diverges  $[0, \beta \rightarrow \infty]$  and the periodic correlation  $C(\tau)$  is expected to have a rapid decay, over a short time-interval, from 1 to its “asymptotic” value, say, at  $\tau = \beta/2$ . Moreover the “regular” part of the correlation, that we define as [38]

$$q_{\text{REG}}(\tau) \equiv C(\tau) - q_{\text{EA}} \quad (45)$$

can be assumed to be small. Therefore we can expand the TAP free-energy in powers of  $q_{\text{REG}}(\tau)$ . Up to terms of the order of  $q_{\text{REG}}(\tau)^3$  we obtain

$$-\frac{\beta F}{N} = \frac{1}{2} \text{Tr} \ln(q_{\text{REG}}(\tau)) + \frac{1}{2\Gamma} \text{Tr} \left( \frac{\partial^2 q_{\text{REG}}(\tau)}{\partial \tau^2} \right) + \frac{\beta}{N} \sum_{i_1 < \dots < i_p} J_{i_1, \dots, i_p} m_{i_1} \dots m_{i_p}$$

$$+\beta \frac{p(p-1)}{4} q_{\text{EA}}^{p-2} \int_0^\beta d\tau q_{\text{REG}}^2(\tau) - \frac{\beta}{2} z (q_{\text{REG}}(0) + q_{\text{EA}} - 1) , \quad (46)$$

where we have focused on the space of time translation invariant (TTI) functions (since the TAP solutions are TTI this does not imply a loss of generality).

Within this approximation the TAP equations become quadratic in Fourier space,

$$1 - \left( \frac{w_k^2}{\Gamma} + z \right) \tilde{q}_{\text{REG}}(\omega_k) + \frac{p(p-1)}{2} q_{\text{EA}}^{p-2} \tilde{q}_{\text{REG}}^2(\omega_k) = 0 , \quad (47)$$

and yield

$$\tilde{q}_{\text{REG}}(\omega_k) = \frac{z + \omega_k^2/\Gamma \pm \sqrt{(z + \omega_k^2/\Gamma)^2 - 2p(p-1)q_{\text{EA}}^{p-2}}}{p(p-1)q_{\text{EA}}^{p-2}} . \quad (48)$$

By taking  $\omega_k = 0$  and comparing to Eq. (38) one obtains

$$\mathcal{E} = -\frac{zq_{\text{EA}}^{1-p/2}}{p} . \quad (49)$$

The spherical constraint reads

$$1 - q_{\text{EA}} = \frac{1}{\beta} \sum_k \tilde{q}_{\text{REG}}(\omega_k) = \int_0^\infty \frac{d\omega}{\pi} \chi''(\omega) \coth\left(\frac{\beta\omega}{2}\right) \quad (50)$$

where

$$\chi''(\omega) \equiv \text{Im } \tilde{q}_{\text{REG}}(\omega_k = -i\omega) = \frac{q_{\text{EA}}^{1-p/2}}{p-1} \sqrt{\mathcal{E}_{\text{TH}}^2 - \left(\mathcal{E} + \frac{\omega^2 q_{\text{EA}}^{1-p/2}}{p\Gamma}\right)^2} . \quad (51)$$

The integral in Eq. (50) has to be taken on the interval  $\omega \in [\omega_-, \omega_+]$  such that the square root is real.

In the low temperature limit, we approximate  $\coth(\beta\omega/2) \sim 1$  and, by changing variables in the integral, we obtain

$$\Gamma I^2(\mathcal{E}, p) = \frac{\pi^2(p-1)^2}{p} (1 - q_{\text{EA}})^2 q_{\text{EA}}^{(p-2)/2} \quad (52)$$

with

$$I(\mathcal{E}, p) = 2 \int_{\sqrt{-\mathcal{E} + \mathcal{E}_{\text{TH}}/2}}^{\sqrt{-\mathcal{E} - \mathcal{E}_{\text{TH}}}} dx \sqrt{\mathcal{E}_{\text{TH}}^2 - (\mathcal{E} + x^2)^2} . \quad (53)$$

Equation (51) yields a relation between  $\Gamma$ ,  $q_{\text{EA}}$  and  $\mathcal{E}$  of the form

$$\Gamma I^2(\mathcal{E}, p) = \text{ct} (1 - q_{\text{EA}})^2 q_{\text{EA}}^{(p-2)/2} , \quad (54)$$

with  $\text{ct}$  a numerical constant. For each  $\mathcal{E}$ , there is a solution with a physically meaningful value of  $q_{\text{EA}}$  that is close to 1, until reaching a critical  $\Gamma_{\text{MAX}}(\mathcal{E})$ . This value tells us when the TAP solutions associated to  $\mathcal{E}$  disappear. It can be easily proven that  $I(\mathcal{E}, p)$  is a growing function of  $\mathcal{E}$ ; hence,  $\Gamma_{\text{MAX}}(\mathcal{E})$  is a decreasing function of  $\mathcal{E}$ . This implies that the TAP solutions that are at the threshold level disappear first than those that are at lower

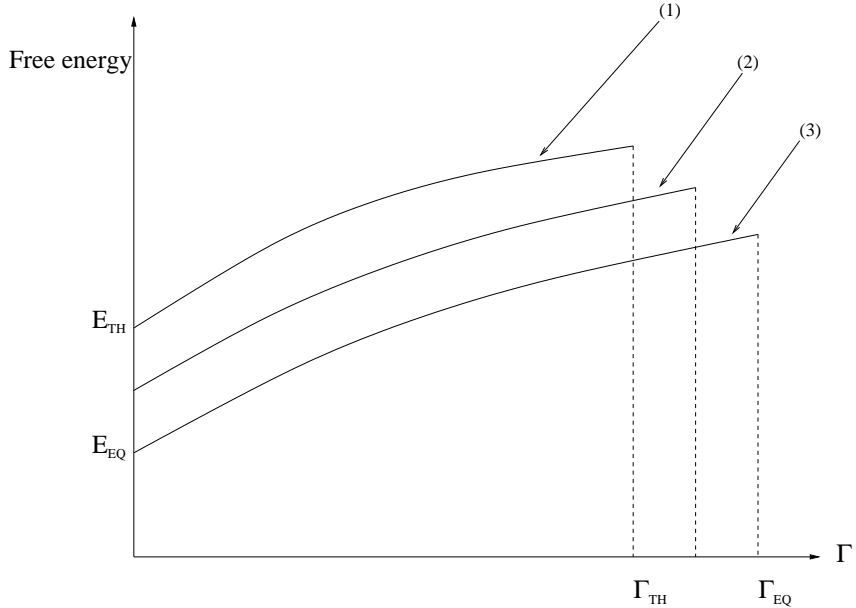


Figure 3: TAP free-energy versus  $\Gamma$  at zero temperature. The curve (1) corresponds to threshold states which are the first ones to disappear at  $\Gamma_{\text{TH}}$ ; the curve (3) corresponds to the states with the lowest free-energy which are the last ones to disappear at  $\Gamma_{\text{RSB}}$  and the curve (2) corresponds to an intermediate state.

values of  $\mathcal{E}$ . This is again similar to the dependence of the classical TAP solutions with temperature [11]: the solutions corresponding to the threshold level disappear at a lower temperature than the ones corresponding to the equilibrium level  $T_{\text{MAX}}(\mathcal{E}_{\text{TH}}) < T_{\text{MAX}}(\mathcal{E}_{\text{EQ}})$  and, more generally,  $T_{\text{MAX}}(\mathcal{E}_1) < T_{\text{MAX}}(\mathcal{E}_2)$  if  $\mathcal{E}_1 > \mathcal{E}_2$ .

The low frequency behavior of the spectral density  $\chi''(\omega) \equiv \text{Im } \tilde{q}_{\text{REG}}(\omega_k = -i\omega)$  of the threshold states is gapless,

$$\chi''(\omega) \sim \omega \quad \text{for } \omega \rightarrow 0^+, \quad (55)$$

whereas all the other states ( $\mathcal{E} < \mathcal{E}_{\text{TH}}$ ) have a gap  $\Delta$  in their excitation spectrum,

$$\chi''(\omega) \sim \sqrt{\omega - \Delta} \quad \text{for } \omega \rightarrow \Delta^+. \quad (56)$$

Furthermore we have studied the dependence of the free-energy on  $\mathcal{E}$  and  $\Gamma$  in the low temperature limit. Plugging the solution (48) into (46) we find, after a tedious computation,

$$-\frac{\beta F}{N} = - \int \frac{d\omega}{\pi\Gamma} \ln \left( 2 \sinh \left( \frac{\beta\omega}{2} \right) \right) \omega \chi''(\omega) + \frac{\beta q_{\text{EA}}^{p/2}}{2} \left( p - 2 - \frac{p}{q_{\text{EA}}} \right) \mathcal{E} \quad (57)$$

where  $q_{\text{EA}}$  satisfies Eq. (38). This expression allows one to study the evolution of the free-energy of the TAP states as a function of  $\Gamma$ . We have found that if one knows a TAP solution at zero temperature and zero  $\Gamma$  one can follow it continuously in  $\Gamma$ . As in the classical case TAP solutions do not cross, merge nor divide in this model.

Figure 3 summarizes these results in a schematic way. Finally, note the special role of the threshold states, which are gapless (contrary to the others), the first ones to disappears and the ones with highest free-energy density.

#### 4.2.4 Stability of TAP states

In the classical case one can check the stability of TAP states. In the quantum case this is a difficult task that has to be performed numerically. In the following we shall limit ourself to prove that the TAP solutions characterized by  $\mathcal{E} = \mathcal{E}_{\text{TH}}$  (threshold states) are characterized by zero modes and are hence marginally stable. We expect that a complete stability analysis will confirm that the TAP states characterized by  $\mathcal{E} < \mathcal{E}_{\text{TH}}$  are stable.

Let us focus on the reduced free-energy Hessian  $\partial^2 F / \partial m_i(\tau) \partial m_j(\tau')$  evaluated in a TAP solution  $\{m_i^\alpha\}$ . This matrix depends on  $\tau, \tau'$  only through their difference. Therefore it is diagonal in Fourier space. Focusing on zero frequency, the original problem reduces to the diagonalization of the following matrix:

$$A_{i,j} = - \sum_{i_3 < \dots < i_p} J_{i,j,i_3, \dots, i_p} m_{i_3}^\alpha \cdots m_{i_p}^\alpha - p\mathcal{E}q_{\text{EA}}^{p/2-1} \delta_{i,j} , \quad (58)$$

where  $q_{\text{EA}} = \sum_i (m_i^\alpha)^2 / N$ . The density of eigenvalues of  $\mathbf{A}$  has been computed in [50] and, except for the isolated eigenvalue corresponding to the eigenvector  $m_i^\alpha$ , it is a semicircular law centered in  $-p\mathcal{E}q_{\text{EA}}^{p/2-1}$  with width  $-p\mathcal{E}_{\text{TH}}q_{\text{EA}}^{p/2-1}$ . Consequently, threshold states are characterized by a vanishing fraction of zero modes.

#### 4.2.5 The classical limit

The classical limit of Eqs. (29) and (30) yields the classical TAP equations computed by Kurchan *et al.* [11]. In fact, in the classical limit,  $C(\tau) = 1$  and the parameter  $z$  is fixed by integrating Eq. (29) between  $0^+$  and  $\beta^+$ . This yields

$$z = \frac{1}{\beta(1-q)} + \frac{p\beta}{2} (1 - q^{p-1}) . \quad (59)$$

By inserting this value of  $z$  in Eq. (30) we obtain

$$\left( \frac{1}{\beta(1-q)} + \frac{p(p-1)\beta}{2} (1 - q) q^{p-2} \right) m_i = p \sum_{i_2 < \dots < i_p} J_{i,i_2, \dots, i_p} m_{i_2} \cdots m_{i_p} , \quad (60)$$

that coincide with the classical TAP equations for the local magnetizations. The equation that fixes  $q_{\text{EA}}$  as a function of  $\mathcal{E}$  in the classical limit is simply obtained from Eq. (34) by setting  $\tilde{C}(0) = 1$ .

### 4.3 Relation between TAP, Matsubara and dynamic approaches

In Section 2 we have recalled the relationship between TAP, replica and dynamical approaches in the classical case. In this Subsection we show how these connections are generalized to quantum systems.

#### 4.3.1 TAP-Matsubara

Via the replica analysis in the Matsubara imaginary-time framework and within a 1step RSB Ansatz, the order parameter is the  $n \times n$  matrix  $Q_{ab}$  which is fully described by:

$n$  identical diagonal elements  $q_d(\tau)$  that depend on the the imaginary time  $\tau$ ,  $n(x^2 - 1)$  constant elements  $q_{\text{EA}}$  that occupy the  $x \times x$  blocks around the diagonal, the remaining  $n^2 - n(x^2 - 1)$  elements  $q_0$  that in the absence of an external field are identically zero. In the  $n \rightarrow 0$  limit, the three parameters  $q_d(\tau)$ ,  $q_{\text{EA}}$  and  $x$ , together with the value of the Lagrange multiplier that enforces the averaged spherical constraint determine the full solution of the problem [38].

The connection between TAP and the Matsubara approaches is obtained by identifying the Edwards-Anderson parameters  $q_{\text{EA}}$  in the two approaches,  $C(\tau)$  with the  $\tau$ -dependent diagonal parameter  $q_d(\tau)$  in  $Q_{ab}$ , and the Lagrange multipliers. In particular we have shown that subtracting the equation obtained for  $a \neq b$  from the one corresponding to  $a = b$  one obtains Eq. (29). In the Matsubara approach one has another equation for  $q_{\text{EA}}$  in which  $x$  acts as an external parameter. Therefore by fixing the value of the breakpoint one fixes the value of  $q_{\text{EA}}$ . As in the classical case two different recipes to fix the breaking point parameter  $x$ , namely optimization and the marginality condition, lead to the static and dynamic transitions, respectively. In the TAP approach the role of  $x$  is played by  $\mathcal{E}$  that enters the equation for  $q_{\text{EA}}$  as a parameter. We have found that the relationship between  $x$  and  $\mathcal{E}$  is encoded in

$$\beta x = \frac{\partial \sigma(\beta, f)}{\partial f} , \quad (61)$$

where  $\sigma$  is the complexity defined in (5), see Appendix B. This suggests that in the a quantum problem the relationship (8) is generalized to

$$\begin{aligned} - \lim_{N \rightarrow \infty} \frac{1}{\beta N} \sum_{\alpha} e^{-\beta x N f_{\alpha}} &= - \lim_{N \rightarrow \infty} \frac{1}{\beta N} \ln \int df e^{N(-\beta x f + \sigma(\beta, f))} \\ &= x \text{Extr}_{q_{\text{EA}}, q_d(\tau)} f_{\text{REP}}(q_{\text{EA}}, q_d(\tau); x, \beta, \Gamma) \end{aligned} \quad (62)$$

Using Eq. (61) we have found that the Matsubara equations for  $q_{\text{EA}}$  and  $q_d(\tau)$  and the TAP equations for  $q_{\text{EA}}$  and  $C(\tau)$  coincide. For instance, the TAP equations for the highest TAP states (threshold states) and the lowest TAP states coincide with the ones obtained in the Matsubara approach by using the marginality condition and the extremization with respect to  $x$ , respectively. Moreover, as another confirmation of Eq. (62) we have verified that the free-energy obtained from the Matsubara computation [38] equals the one obtained in the TAP approach for all values of  $\beta$  and  $\Gamma$ . In other words, we have checked that

$$-\beta F = \ln \sum_{\alpha} e^{-\beta F_{\alpha}} . \quad (63)$$

As a consequence the phase diagram that follows from the TAP approach coincides with the one obtained in [38].

#### 4.3.2 TAP-out of equilibrium dynamics

The study of the real-time dynamics of the p-spin quantum model evolving in contact with an Ohmic quantum environment has been performed in [37]. The dynamical behavior is characterized by two regimes. At high temperature and high  $\Gamma$  the system equilibrates in the paramagnetic state via an equilibrium dynamics. Whereas at low temperature and

low  $\Gamma$  the system ages and remains out of equilibrium also at infinite times. As in the classical case we have found that the long-time out of equilibrium dynamics is dominated by the threshold states. This is proven by the fact that the equations for  $q_{\text{EA}}$  and  $C(\tau)$  within the TAP approach coincide with the ones obtained from the study of the real-time dynamics, when the following limits are taken in its precise order:  $\lim_{\gamma \rightarrow 0} \lim_{t \rightarrow \infty} \lim_{N \rightarrow \infty}$ . In other words, when one takes first the thermodynamic limit, next the long-time limit of the system's dynamics in contact with the environment and, finally, the strength of the coupling to the environment  $\gamma$  to zero. Notice that this equivalence holds for the paramagnetic states also. Finally, we have shown that the relationship between the effective temperature [53] arising in the asymptotic out of equilibrium regime [37] and the complexity is, as classically,

$$\frac{1}{T_{\text{EFF}}} = \left. \frac{\partial \sigma(\beta, f)}{\partial f} \right|_{f=f_{\text{TH}}}. \quad (64)$$

Note that the connection between TAP and real-time dynamics is done by identification of several equations. A more precise analysis, along the lines of [24], should prove the full equivalence of the two methods.

## 5 The phase diagram of discontinuous glassy systems

In this section we present some general arguments that allow one to predict the phase diagram of discontinuous glassy systems. Since the free-energy landscape plays a key role, we expect these results to have a certain degree of universality and to apply to this entire class of disordered systems.

### 5.1 The static transition

Let us focus on two limiting regions of the phase diagram: around the classical phase transition ( $\Gamma = 0$ ) and around the quantum phase transition ( $T = 0$ ).

In the former case the physics is well known and it is reviewed in Section 2. The effect of switching on weak quantum fluctuations consists only in a weak variation of the complexity  $\sigma$ . For this reason the effect of quantum fluctuations reduces simply to a variation of the thermodynamic ( $T_s$ ) and the dynamic ( $T_d$ ) transition temperatures (respectively lines (1) and (3) in Fig. 4).

At zero temperature and low  $\Gamma$  the system is in the glassy phase (GP), whereas at very high  $\Gamma$  quantum fluctuations destroy the glassy phase and the system is a quantum paramagnet (QPM). As a consequence one expects that a quantum phase transition should divide these two regimes at a certain value  $\Gamma_c$ .

At zero temperature the complexity is expected to remain a smooth function of the free-energy density<sup>4</sup>. Consequently, equation (4) implies that the sum over the exponential number of glassy states is always dominated by the lowest ones in free-energy since the  $\beta f$  term in the exponential largely dominates in this limit (this is different from the classical problem in which other states dominate between  $T_s$  and  $T_d$ ). At zero temperature these

---

<sup>4</sup>For instance the complexity does not blow up for  $T \rightarrow 0$  since it is bounded by the logarithm of the number of energy minima divided by  $N$ , which is a finite quantity independent of temperature.

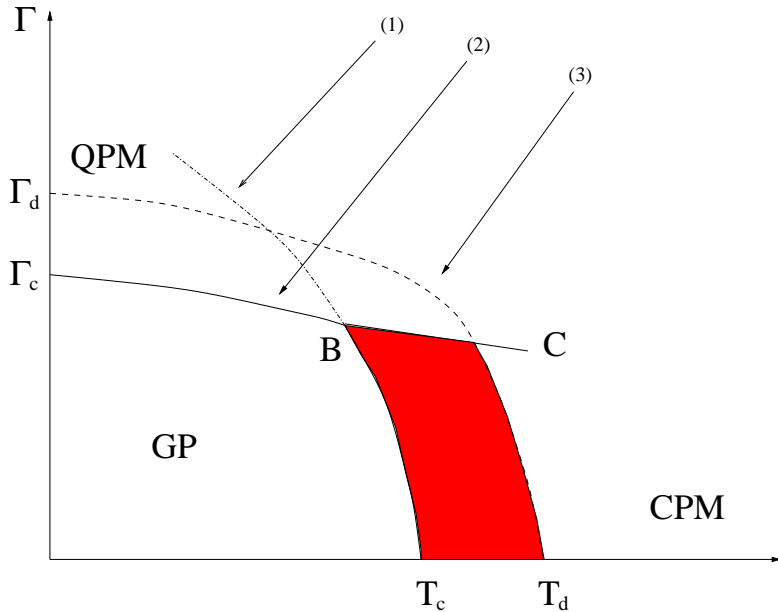


Figure 4: A schematic representation of the phase diagram which is expected to be generic for systems having a discontinuous transition in the classical limit. The line (1), from  $(T_c, 0)$  to the point B, represents the static transition between the classical paramagnet (CPM) and the glassy phase (GP). The region in red between the lines (1) and (3) is the phase in which the CPM is fractured into an exponential number of TAP states. The line (2) from the point B to  $(\Gamma_c, 0)$ , signals the static transition between the quantum paramagnet (QPM) and the GP. The line (3) indicates the dynamic transition  $T_d$  as a function of  $\Gamma$ .

are the states with lower angular potential energy, *i.e.* with  $\mathcal{E} = \mathcal{E}_{\text{EQ}}$ . Now, from Fig. 2 we conclude that  $\sigma(\mathcal{E}_{\text{EQ}}) = 0$  at zero temperature and for all  $\Gamma$ . For this reason the mechanism behind the transition must be totally different from the classical one. The transition cannot be related to a configurational entropy that vanishes when approaching  $\Gamma_c$  from above (“entropy crisis”) since this quantity is always zero at zero temperature.

Indeed, according to Eq. (61), if we assume that  $\partial\sigma(\beta, f)/\partial f < +\infty$  when  $T \rightarrow 0$ , then  $x \rightarrow 0$  for all  $\Gamma$  in the glassy phase. In the paramagnetic phase instead  $x = 1$ . Thus,  $x$  must jump at the transition. If the Edwards-Anderson parameter also jumps at  $\Gamma_c$ , the susceptibility is discontinuous, and the transition is of first order thermodynamically. As in the previous case the effect of switching on thermal fluctuations reduces simply, for low  $T$ , to a variation of  $\Gamma_c$  (line (2) in Fig. 4).

Another hint on the difference between classical and quantum phase transition can be gained by a technical remark. It is well known that the paramagnetic solution of the classical problem remains stable in the low temperature phase. This is a spurious solution of the mean field equations which has to be discarded in the analysis of the low temperature regime. In the quantum case, one also expects to find a spurious paramagnetic solution, which is the continuation of the classical paramagnet to low temperatures. This solution exists to the left of line (1) in Fig. 4, consequently one expects coexistence of two paramagnetic solutions: a physical one which is the continuation of the quantum paramagnet

valid at low temperatures and high  $\Gamma$  and a spurious one which is the continuation of the classical paramagnet.

In the classical case the transition is of second order even if the order parameter jumps discontinuously. This peculiar behavior is due to the fact that near the transition the paramagnetic state is fractured into an exponential number of states which continuously become the ones responsible for the glassy phase at low temperature. This is not possible at zero temperature (the quantum paramagnet is not formed by a collection of glassy states) and therefore it is reasonable to expect a quantum first order phase transition between the glass phase and the quantum paramagnet.<sup>5</sup>

Finally, note that  $F_{\text{QPM}} = F_{\text{GP}} = F_{\text{CPM}}$  on the point B. We then expect that a first order transition line separating the QPM from the CPM starts at this point. This line should end on a point C given that for very large value of  $\Gamma$  and  $T$  the quantum and thermal fluctuations are so strong that the system becomes non interacting and in this case only one paramagnetic phase exists. In the analysis of the  $p = 3$  spherical spin-glass model [38] the line BC has not been found. We conjecture that in this case the line BC is so short that it is very difficult to find numerically. Furthermore, within the accuracy of the algorithm, the dynamic and static critical lines collapse at the point B. In the quantum model studied in [36] instead this line has been detected and it was demonstrated in this paper that its length increases with  $p$ .

## 5.2 The dynamic transition

Now that the equilibrium phase diagram is completely predicted from a qualitatively point of view, we can focus on the non-equilibrium regime. As noted previously, low quantum fluctuations simply change the values of  $T_d$  but do not change qualitatively the dynamic transition which remains second order in the sense that the asymptotic energy is continuous across the transition, but its derivative is not. This remains true until the line (2) reaches the line BC. After this point the dynamic transition between the the quantum paramagnet and the threshold states becomes first-order, i.e. the asymptotic energy is not continuous across the transition. This, of course, is very difficult to see numerically since the discontinuity has a very small value.

## 5.3 Summary

In summary, through some general arguments based on the TAP approach we have predicted a phase diagram that should have a certain degree of universality since its form is determined by the qualitative form of the free-energy landscape. Indeed, not only the quantum  $p$  spin spherical model exhibits the phase diagram displayed in Fig. 4 but some other classical and quantum models share exactly the organization of phases and transitions [15, 16, 36, 45].

---

<sup>5</sup>Note however that other scenarios are possible. For example the number of glassy states could diminish when  $\Gamma$  increases and vanish exactly at  $\Gamma_c$ . In this case the glassy states could be grown up continuously from the quantum paramagnet.

## 6 Conclusion

In this paper we have derived TAP equations for a large class of mean field disordered quantum system. Moreover we have applied the TAP approach to the quantum version of the spherical  $p$  spin model. The study of this system, whose real-time dynamics and statics have been analyzed in [37, 38], has furnished an ideal benchmark to generalize to the quantum case several concepts developed for classical disordered systems. Armed with this knowledge, founded on the study of the free-energy landscape, we have shown that the same phase diagram, presented in Fig. 4, naturally emerges in a large class of quantum disordered systems, those having a classical discontinuous transition.

Whether other models like the SK model in a transverse field, or its soft spin version studied in [39], also have such crossover in the transition from the disordered to the ordered phase is an issue that deserves revision. For the moment, no study of models with classical continuous transition has shown this feature. However, it might have been masked by the methods used in previous studies. The soft SK model might be the easiest example where to answer this question via, *e.g.*, a careful application of the replicated Matsubara approach.

We would like to stress that the TAP approach furnishes an alternative and more transparent route to replicas which has also the advantage of showing explicitly the weakness of the mean field description. Let us cite one example. The marginality prescription in the replica approach becomes the more transparent statement that the non-equilibrium dynamics is dominated by the TAP states which are marginally stable, *i.e.* the flatness of the free-energy landscape around these states is responsible for aging. Concerning one of the weaknesses of the mean field description we would like to underline that the enormous number of pure states (with different free-energy densities) found for mean field models cannot persist in finite dimensions and the majority of them should become *metastable* states. How this changes the mean field scenario is an active domain of research for classical systems [54].

We remark that interesting continuations of our work concern, on the one hand, the application of the TAP approach to different quantum mean-field models [31, 33, 34] and, on the other hand, the generalization of the static quantum TAP approach to real-time dynamics (for classical systems this has been done in [24]). This would allow one to show the relationship between long-time dynamics and free-energy landscape for quantum systems directly. Finally, the precise definition of a “quantum state” is a delicate matter and merits further analysis. In this paper we have simply called “state” a minimum of the TAP free-energy density. One possible way to verify the existence and stability of these states is by studying the dynamics of this system starting from particular initial conditions as done in [48, 49] for the classical model. This study is underway [55].

**Acknowledgments** We wish to thank D. R. Grempel, J. Kurchan, G. Lozano and C. A. da Silva Santos for very useful discussions. G. B. is supported by the Center of Material Theory, Rutgers University, NJ, USA. L. F. C. thanks ECOS-Sud for a travel grant

and financial support from the grant “Algorithmes d’optimisation et systèmes quantiques désordonnés”, ACI-Jeunes Chercheurs, 2000.

## Appendix A

In this appendix we show that the equation for  $q_{\text{EA}}$  that leads to a solution with the correct physical properties is Eq. (34) with the minus sign. Indeed, we search a solution that corresponds to a minimum of the TAP free-energy. The full stability analysis, that involves the evaluation of the complete Hessian of the TAP free-energy, is rather hard and has to be done numerically (for instance, the form of  $\tilde{C}(\omega)$  can only be obtained numerically).

However, we can still perform a partial analysis that suffices to justify the choice of the minus sign. Let us concentrate on the following diagonal elements of the Hessian:

$$\frac{\delta(-\beta F)}{\delta q_{\text{EA}}^2} = -\frac{1}{2} \left[ \left(1 - \frac{p}{2}\right) \tilde{C}(0) + \frac{p}{2} \beta q_{\text{EA}} \right] \left[ \frac{1}{(\tilde{C}(0) - \beta q_{\text{EA}})^2 q_{\text{EA}}} - \frac{p(p-1)}{2} q_{\text{EA}}^{p-3} \right] \quad (65)$$

$$\frac{\partial(-\beta F)}{\partial \tilde{C}(0) \partial \tilde{C}(0)} = \frac{-1}{(\tilde{C}(0) - q\beta)^2} + \frac{p(p-1)}{2\beta} \int_0^\beta d\tau C^{p-2}(\tau) . \quad (66)$$

From  $z_\pm$ ’s definition we find

$$z_- \leq \frac{-\mathcal{E}_{\text{TH}}}{p-1} , \quad z_+ \geq \frac{-\mathcal{E}_{\text{TH}}}{p-1} . \quad (67)$$

Since  $q_{\text{EA}}$  is fixed by Eq. (34), the second factor on the right-hand-side of Eq. (65) is positive (negative) for  $z_-$  ( $z_+$ ). A stable solution corresponds to a negative value of (65) and (66), therefore one has to take the solution  $q''$  for  $z_-$  and  $q'$  for  $z_+$ . Moreover, since for  $\mathcal{E} < \mathcal{E}_{\text{TH}}$  the right hand side of (34) is positive then we obtain that  $\tilde{C}(0) - \beta q'$  and  $\tilde{C}(0) - \beta q''$  are positive and using that

$$\left( \frac{1}{\beta} \int_0^\beta C^\alpha(t) dt \right) \geq \left( \frac{1}{\beta} \int_0^\beta C(t) dt \right)^\alpha \quad \alpha > 1$$

and imposing that (66) has to be negative, we obtain:

$$\frac{1}{(\tilde{C}(0) - \beta q_{\text{EA}})^2} - \frac{p(p-1)}{2} q_{\text{EA}}^{p-2} \geq 0 \quad \text{for } q = q', q''$$

But this is impossible for  $z_+$ , i.e. it is not possible to have a consistent stable  $z^+$  solution.

## Appendix B

In this Appendix we give an argument in favor of the relation  $\beta x = \partial\sigma(\beta, f)/\partial f$  in Eq. (61). Let us start by assuming that it does hold and see that it leads to the equation linking  $x$ ,  $q_{\text{EA}}$  and  $C(\tau)$  in the Matsubara approach. First of all we write the derivative of  $\sigma$  with respect to  $f$  as a derivative with respect to  $\mathcal{E}$ . This can be easily done by noticing that differentiating  $f$  in Eq. (13) with respect to  $\mathcal{E}$  at  $\beta$  and  $\Gamma$  fixed is equivalent to differentiating  $f$  with respect to  $\mathcal{E}$  at  $\beta$ ,  $\Gamma$ ,  $q_{\text{EA}}$  and  $C(\tau)$  fixed because  $f$  is stationary in  $q_{\text{EA}}$  and  $C(\tau)$ . As a consequence we find

$$\beta x = \frac{\partial\sigma}{\partial f} = \frac{\partial\sigma}{\partial\mathcal{E}} \frac{\partial\mathcal{E}}{\partial f} = \frac{\partial\sigma}{\partial\mathcal{E}} q_{\text{EA}}^{-p/2}. \quad (68)$$

The derivative  $\partial\sigma/\partial\mathcal{E}$  can be easily computed from Eq. (44). One arrives at

$$\frac{p}{2} = \left( \tilde{C}(0)^2 - \beta^2 q_{\text{EA}}(x-1) + \beta q_{\text{EA}} \tilde{C}(0)(x-2) \right)^{-1}. \quad (69)$$

In summary, starting from the TAP approach at fixed  $\mathcal{E}$  we obtain  $q_{\text{EA}}$  and  $C(\tau)$ . Assuming then that Eq. (61) holds we obtain the equation linking  $q_{\text{EA}}$  and  $x$  in the Matsubara approach. The equations for  $C(\tau)$  in the TAP and Matsubara approaches, once  $q_{\text{EA}}$  is fixed, are identical. Hence we have proven that Eq. (61) leads to the Matsubara results in [38].

The proof will be complete if we showed the other sense of the implication.

## References

- [1] D. J. Thouless, P. W. Anderson and R. Palmer, Phil. Mag. **35**, 593 (1977).
- [2] C. de Dominicis, M. Gabay, T. Garel and G. Toulouse, J. Phys. **41**, 923 (1980).
- [3] A. J. Bray and M. A. Moore, J. Phys. **C13**, L469 (1980).
- [4] In J. Kurchan, J. Phys. **I** it is shown that there is a problem with the calculation in [3] since, for topological reasons, the number of TAP solutions computed should actually be one. Two solutions to this puzzle have been proposed, one in this article and another one in [13].
- [5] T. Plefka, J. Phys. **A15**, 1971 (1982).
- [6] A. Georges and J. S. Yedidia, J. Phys. **A24**, 2173 (1991).
- [7] C. de Dominicis and A. P. Young, J. Phys. **A16**, 2063 (1983).
- [8] M. Mézard, G. Parisi and M. A. Virasoro, *Spin glass theory and beyond* (Singapore: World Scientific) 1987.
- [9] T. R. Kirkpatrick and P. Wolynes, Phys. Rev. **A35**, 3072 (1987), Phys. Rev. **B36**, 8552 (1987).
- [10] H. Rieger, Phys. Rev. **B 46**, 14655 (1992).

- [11] J. Kurchan, G. Parisi and M. A. Virasoro, J. Phys. (France) I **3**, 1819 (1993).
- [12] A. Crisanti and H-J Sommers, J. Phys. I France **5**, 805 (1995).
- [13] A. Cavagna, I. Giardina and G. Parisi, Phys. Rev. **B57**, 11251 (1998).
- [14] A. Cavagna, J. P. Garrahan and I. Giardina, J. Phys. **A32**, 711 (1999).
- [15] S. K. Ghatak and D. Sherrington, J. Phys. **C10**, 3149 (1977).
- [16] P. J. Mottishaw and D. Sherrington, J. Phys. **C18**, 5201 (1985).
- [17] T Yokota, J. Phys. **C4**, 2615 (1992).
- [18] M. Rehker and R. Oppermann, J. Phys. **C11**, 1537 (1999).
- [19] F. A. da Costa and J. M. de Araújo, Eur. Phys. J. **B 15**, 313 (2000).
- [20] J-P Bouchaud, L. F. Cugliandolo, J. Kurchan and M. Mézard, *Out of equilibrium dynamics in spin glasses and other glassy systems*, in *Spin-glasses and random fields*, A. P. Young ed. (World Scientific, 1998).
- [21] E. Vincent, J. Hammann, M. Ocio, J-P Bouchaud and L. F. Cugliandolo, *Slow dynamics and aging in glassy systems*, in *Sitges 1996*, ed. M. Rubí (Springer-Verlag, 1997). P. Nordblad and P. Svendlidh, *Experiments on spin-glasses in Spin-glasses and random fields*, A. P. Young ed. (World Scientific, 1998).
- [22] L. F. Cugliandolo and J. Kurchan, Phys. Rev. Lett. **71**, 173 (1993), Phil. Mag. **B71**, 501 (1995).
- [23] L. F. Cugliandolo and J. Kurchan, J. Phys. **A27**, 5749 (1994).
- [24] G. Biroli, J. Phys. **A32**, 8365 (1999).
- [25] W. Wu, B. Ellmann, T. F. Rosenbaum, G. Aeppli and D. H. Reich, Phys. Rev. Lett. **67**, 2076 (1991). W. Wu, D. Bitko, T. F. Rosenbaum and G. Aeppli, Phys. Rev. Lett. **71**, 1919 (1993). T. F. Rosenbaum, J. Phys. **C8**, 9759 (1996). J. Brooke *et al*, Science **284**, 779 (1999).
- [26] E. Courtens, J. Phys. Lett. (Paris) **43** L199 (1982), Phys. Rev. Lett. **52** 69 (1984). E. Matsushita and T. Matsubara, Prog. Theor. Phys. **71** 235 (1984). R. Pirc, B. Tadic and R. Blinc, Z. Phys. **B61** 69 (1985), Phys. Rev. **B36** 8607 (1987).
- [27] Z. Ovadyahu, A. Vaknin and M. Pollack, Phys. Rev. Lett. **84**, 3402 (2000).
- [28] D. J. Scalapino, Phys. Rep. **250**, 329 (1995).
- [29] S. Rogge, D. Natelson and D. D. Osheroff, Phys. Rev. Lett. **76**, 3136 (1996). S. Rogge, D. Natelson, B. Tigner and D. D. Osheroff, Phys. Rev. **B55**, 11256 (1997). D. Natelson, D. Rosenberg and D. D. Osheroff, Phys. Rev. Lett. **80**, 4689 (1998).

- [30] A. J. Bray and M. A. Moore, J. Phys. **C13**, L655 (1980).
- [31] P. Shukla and S. Singh, Phys. Lett. **A81**, 477 (1981). T. Yamamoto and H. Ishii, J. Phys. **C20**, 6053 (1987). V. Dobrosavljevic and D. Thirumalai, J. Phys. **A23** L767, (1990). J. Miller and D. A. Huse, Phys. Rev. Lett. **70**, 3147 (1993). Y. Y. Goldschmidt, Phys. Rev. **B41**, 4858 (1990). T. Kopeć, Phys. Rev. **B52**, 9590 (1995). T. Giamarchi and P. Le Doussal, Phys. Rev. **B53** 15206 (1996). D. R. Grempel and M. J. Rozenberg, Phys. Rev. Lett. **80**, 389 (1998); *ibid* **81**, 2550 (1998). A. Georges, O. Parcollet and S. Sachdev, Phys. Rev. Lett. **85**, 840 (2000).
- [32] H. Ishii and T. Yamamoto, J. Phys. **C18**, 6225 (1985).
- [33] Y. Ye, N. Read and S. Sachdev, Phys. Rev. Lett. **70**, 4011 (1993). N. Read, S. Sachdev and Y. Ye, Phys. Rev. **B52**, 384 (1995).
- [34] L. De Cesare, K. Lukierska-Walasek, I. Rabuffo and K. Walasek, Physica **A214**, 499 (1995), J. Phys. **A29**, 1605 (1996).
- [35] L. De Cesare, K. Lukierska-Walasek and K. Walasek, Phys. Rev. B **45**, 8127 (1992).
- [36] T. M. Nieuwenhuizen and F. Ritort, Physica **A250**, 89 (1998).
- [37] L. F. Cugliandolo and G. Lozano, Phys. Rev. Lett. **80**, 4979 (1998); Phys. Rev. **B59**, 915 (1999).
- [38] L. F. Cugliandolo, D. R. Grempel and C. A. da Silva Santos, Phys. Rev. Lett. (2000) and in preparation.
- [39] M. Kennett and C. Chamon, cond-mat/0009099.
- [40] D. S. Fisher, Phys. Rev. Lett. **69**, 534 (1992). F. Igloi and H. Rieger, Phys. Rev. **B57**, 11404 (1998). M. Y. Guo, R. N. Bhatt and D. A. Huse, Phys. Rev. Lett. **72**, 4137 (1994). H. Rieger and A. P. Young, Phys. Rev. Lett. **72**, 4141 (1994). A. H. Castro Neto and B. A. Jones, cond-mat/0003085. O. Motrunich, K. Damle, D. A. Huse, Phys. Rev. Lett. **84**, 3434 (2000) and cond-mat/0005543.
- [41] A. Crisanti and H-J Sommers, Z. Phys. **B87**, 341 (1992).
- [42] B. Derrida, Phys. Rev. **B24**, 1613 (1981). D. J. Gross and M. Mézard, Nucl. Phys. **B240** [FS], 431 (1984).
- [43] T. R. Kirkpatrick and D. Thirumalai, Phys. Rev. **B36**, 5388 (1987), Phys. Rev. **B38**, 4881 (1988).
- [44] P. Mottishaw, Europhys. Lett. **1**, 409 (1986).
- [45] R. Oppermann and B. Rosenow, Phys. Rev. **B60**, 10325 (1999) and refs. therein.
- [46] H. Feldmann and R. Oppermann, J. Phys. **33**, 1325 (2000).
- [47] R. Monasson, Phys. Rev. Lett. **75**, 2847 (1995).

- [48] A. Barrat, R. Burioni, M. Mézard, *J. Phys. A* **29**, 1311 (1996).
- [49] S. Franz and G. Parisi, *J. Phys. I (France)* **5**, 1401 (1995).
- [50] A. J. Bray and M. A. Moore, *J. Phys. C* **12**, L441 (1979).
- [51] T. R. Kirkpatrick and D. Thirumalai, *Phys. Rev. Lett.* **58**, 2630 (1987), *Phys. rev. B* **36**, 5388 (1987).
- [52] A. Georges, G. Kotliar, W. Krauth and M.J. Rozenberg *Rev. Mod. Phys.* **68**, 13 (1996).
- [53] L. F. Cugliandolo, J. Kurchan and L. Peliti, *Phys. Rev. E* **55**, 3898 (1997).
- [54] G. Biroli and J. Kurchan, *cond-mat/0005499*.
- [55] L. F. Cugliandolo, D. R. Grempel, C. A. da Silva Santos, in preparation.